Absorption, Fluorescence, and Magnetic Circular Dichroism Spectra of and Molecular Orbital Calculations on Tetrabenzotriazaporphyrins and Tetranaphthotriazaporphyrins

John Mack,[†] Nagao Kobayashi,*[,‡] Clifford C. Leznoff,[§] and Martin J. Stillman*[,†]

Department of Chemistry, The University of Western Ontario, London, Ontario, Canada N6A 5B7, and Faculty of Graduate Science, Tohoku University, Sendai, Japan

Received November 20, 1996[⊗]

Extensive analyses of the electronic absorption, magnetic circular dichroism (MCD), and fluorescence emission and excitation spectra of peripherally-substituted tetrabenzotriazaporphyrin (TBTrAP) and tetranaphthotriazaporphyrin (TNTrAP) complexes are reported. ZINDO calculations of the UV−visible absorption spectra of free base and dianionic (deprotonated) TBTrAP and TNTrAP complexes are described. The optical spectra of TBTrAP and TNTrAP are assigned on the basis of molecular orbital (MO) calculations using the ZINDO program and the theory that has been developed previously to account for the spectral properties of porphyrin and phthalocyanine complexes. Analysis of the absorption and MCD spectra of the ring-reduced anion radical species of Pc and TBTrAP complexes shows that the optical spectra of $[TBTrAP(-3)]^-$ are markedly different from those of analogous Pc species. EPR signals observed at 77 K for Pc(−3) radical species provide evidence for a doublet ground state, while the absence of an EPR signal for $[TBTrAP(-3)]^-$ indicates that the species dimerizes upon reduction. The absorption and MCD spectra of the dimeric $[TBTrAP(-3)]^-$ species are found to be consistent with the band assignment developed previously to account for the spectral properties of main group Pc anion radicals.

Introduction

Metal porphyrin complexes (MP(−2)) play a vital role in biological processes such as photosynthesis and respiration.[1] These complexes offer a unique chemistry that has a great many possible industrial applications. Perhaps the most commercially important group of the porphyrin class of molecules is the phthalocyanines, known systematically as tetrabenzo[5,10,15,20]-tetraazaporphyrins.[2] Metal phthalocyanine complexes (MPc(−2)) have traditionally found use as dyes and pigments and, more recently, as the photoconducting agent in photocopiers, because of their easy synthesis, high thermal stability, and the presence of intense $\pi \rightarrow \pi^*$ transitions in the visible region.[3] There has been renewed interest in the use of phthalocyanines in a variety of high-technology fields, including use in semiconductor devices,[4] photovoltaic and solar cells,[5] electrophotography,[6] rectifying devices,[7] molecular electronics,[8] Langmuir−Blodgett films,[9] electrochromism in display devices,[10] low-dimensional metals,[11] gas sensors,[12] liquid crystals,[13] and nonlinear optics[14] and as photosensitizers[15] and electrocatyltic agents.[16] In many of these applications, the exact wavelength of the major $\pi \rightarrow \pi^*$ transitions in either the visible or UV region is of critical importance. Since it is impossible, however, to find a single phthalocyanine complex to absorb significantly for all wavelengths, there is considerable current interest in the electronic spectroscopy of structurally modified phthalocyanine molecules that exhibit major absorption bands at a variety of wavelengths from the near-IR to the UV regions.[17−19] A detailed understanding of how the electronic structure of

* To whom correspondence should be addressed. Fax: (519) 661-3022. Tel: (519) 661-3821. Internet: Stillman@uwo.ca.
† University of Western Ontario.
‡ Tohoku University.
§ York University.
⊗ Abstract published in *Advance ACS Abstracts,* October 1, 1997.

(1) (a) *The Porphyrins*; Dolphin, D., Ed.; Academic Press: New York, 1978. (b) *Ann. New York Acad. Sci.* **1973**, 206.
(2) (a) *Phthalocyanine. Principles and Properties*; Leznoff, C. C., Lever, A. B. P., Eds.; VCH Publications: New York, 1989; Vol. 1. (b) *Phthalocyanine. Principles and Properties*; Leznoff, C. C., Lever, A. B. P., Eds.; VCH Publications: New York, 1993; Vol. 2. (c) *Phthalocyanine. Principles and Properties*; Leznoff, C. C., Lever, A. B. P., Eds.; VCH Publications: New York, 1993; Vol. 3.
(3) (a) Stillman, M. J.; Nyokong, T. In *Phthalocyanine. Principles and Properties*; Leznoff, C. C., Lever, A. B. P., Eds.; VCH Publications: New York, 1993; Vol. 1, Chapter 3, pp 133−290. (b) Stillman, M. J. In *Phthalocyanine. Principles and Properties*; Lever, A. B. P., Leznoff, C. C., Eds.; VCH Publications: New York, 1993; Part 3, Chapter 5, pp 227−296.
(4) Simon, J.; Andre, J.-J. *Molecular Semiconductors*; Springer: Berlin, 1985; Chapter 3.
(5) Tang, C. W. *Appl. Phys. Lett.* **1986**, *60*, 1047.
(6) Loutfy, R. O.; Hor, A. M.; Hsiao, C. K.; Baranyi, G.; Kazmaier, P. *Pure Appl. Chem.* **1988**, *60*, 1047.
(7) Abe, K.; Sato, H.; Kimura, T.; Ohkatsu, Y.; Kusano, T. *Makromol. Chem.* **1989**, *190*, 2693.
(8) Simic-Glavaski, B. In *Phthalocyanine. Principles and Properties*; Leznoff, C. C., Lever, A. B. P., Eds.; VCH Publications: New York, 1993; Vol. 3, Chapter 3, pp 119−166.
(9) (a) Roberts, G. G.; Petty, M. C.; Baker, S.; Fowler, M. T.; Thomas, N. J. *Thin Solid Films* **1985**, *132*, 113. (b) Cook, M. J.; Dunn, A. J.; Daniel, M. F.; Hart, R. C. O.; Richardson, R. M.; Roser, S. J. *J. Chem. Soc., Dalton Trans.* **1988**, 1583. (c) Palacin, S.; Lesieur, P.; Stefanelli, I.; Barraud, A. *Thin Solid Films* **1988**, *159*, 83.
(10) Nicholson, M. M. In *Phthalocyanine. Principles and Properties*; Leznoff, C. C., Lever, A. B. P., Eds.; VCH Publications: New York, 1993; Vol. 3, Chapter 2, pp 71−118.
(11) (a) Marks, T. J. *Angew. Chem., Int. Ed. Engl.* **1990**, *29*, 857. (b) Hanack, M.; Datz, A.; Fay, R.; Fischer, K.; Keppeler, U.; Koch, J.; Metz, J.; Mezger, M.; Schneider, O.; Schulze, H. J. In *Handbook of Conducting Polymers*; Skotheim, T. A. B., Ed.; Marcel Dekker: New York, 1986; Vol. 1, Chapter 5, p 133.
(12) Snow, A. W.; Barger, W. R. In *Phthalocyanine. Principles and Properties*; Leznoff, C. C., Lever, A. B. P., Eds.; VCH Publications: New York, 1989; Vol. I, Chapter 3, pp 341−392.
(13) (a) Van der Pol, J. F.; Neeleman, E.; Zwikker, J. W.; Nolte, R. J. M.; Drenth, W.; Aerts, J.; Visser, R.; Picken, S. *J. Liq. Cryst.* **1989**, *6*, 577. (b) Simon, J.; Sirlin, C. *Pure Appl. Chem.* **1989**, *61*, 1625.
(14) (a) Casstevens, M. K.; Samoc, M.; Pfleger, J.; Prasad, P. M. *J. Chem. Phys.* **1990**, *92*, 2019. (b) Simon, J.; Bassoul, P.; Norvez, S. *New J. Chem.* **1989**, *13*, 13.
(15) Kato, M.; Nishioka, Y.; Kaifu, K.; Kawamura, K.; Ohno, S. *Appl. Phys. Lett.* **1985**, *46*, 196.
(16) Lever, A. B. P.; Hempstead, M. R.; Leznoff, C. C.; Lin, W.; Melnik, M.; Nevin, W. A.; Seymour, P. *Pure Appl. Chem.* **1986**, *18*, 1467.

S0020-1669(96)01389-4 CCC: $14.00

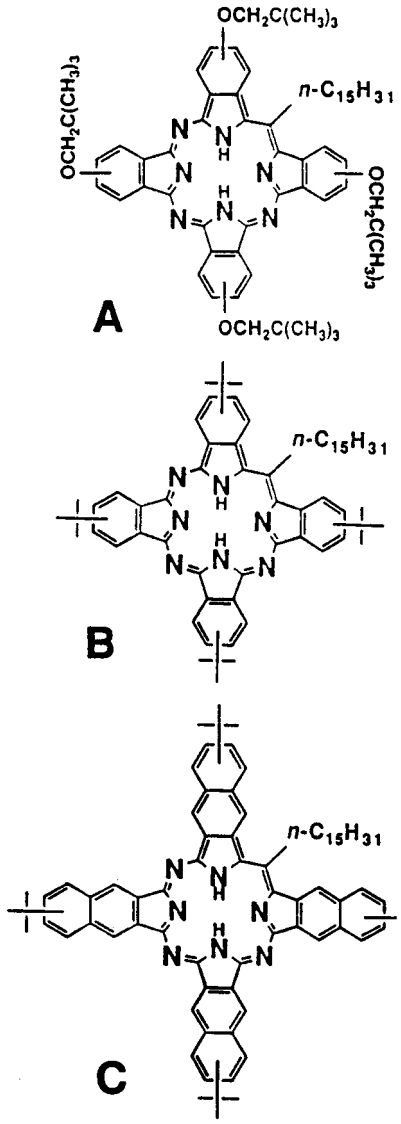

Figure 1. Molecular structures of pentadecyl-substituted compounds, **A**, tetraneopentoxytetrabenzo[5,10,15]triazaporphyrin, **B**, tetra-*tert*-butyltetrabenzo[5,10,15]triazaporphyrin, **C**, and tetraneopentoxytetranaphtho[5,10,15]triazaporphyrin.

structurally modified MPc(−2) complexes depends on the structural changes will aid in the development of new industrial applications for these molecules.

Electronic Structure of Tetrabenzotriazaporphyrins and Related Compounds

The molecular structures of the compounds studied are shown in Figure 1. The tetrabenzo[5,10,15]triazaporphyrins (TBTrAP) **A** and **B** differ only in their peripheral *tert*-butyl and neopentoxy substituent groups. In compound **C** the fused benzene rings of compound **B** are replaced with fused *tert*-butylated naphthalene ring systems to form tetranaphtho[5,10,15]triazaporphyrin (TNTrAP). Peripheral substitution with the *tert*-butyl and neopentoxy groups has little impact on the optical spectra and helps to enhance greatly the solubility of phthalocyanines and related complexes in optically transparent solvents.[3a]

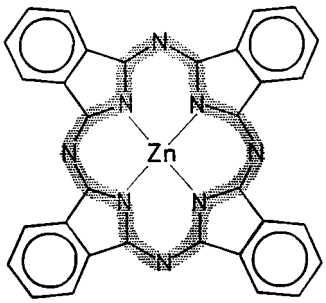

Figure 2. Molecular structure of a typical main group metal phthalocyanine showing the path of the 16-membered cyclic polyene ring that forms the basis of the 4-orbital calculations of Gouterman used to account for the two lowest energy $\pi \rightarrow \pi^*$ transitions in porphyrins and phthalocyanines.

In its simplest description, the electronic structure of MPc(−2) complexes can be viewed as a 16-atom, 18-π-electron aromatic system that runs around the inner perimeter of the ligand, Figure 2. Gouterman's model, based on a 4-orbital linear combination of atomic orbitals (LCAO), has been widely used to describe the optical spectra of both MP(−2) and MPc(−2) complexes.[3,22−26] The ideal 16-atom cyclic polyene is distorted by the presence of the four pyrrole nitrogen atoms so that the symmetry is reduced to D_{4h} and a slight lifting of the orbital degeneracy of the ungerade molecular orbitals takes place; see Figure 3. The HOMO has an M_L value of ±4 while the LUMO has an M_L value of ±5. This simple scheme gives rise to an allowed B transition ($\Delta M_L = \pm 1$) and a forbidden Q transition ($\Delta M_L = \pm 9$). Gouterman's group demonstrated the validity of the 4-orbital approach through more complex molecular orbital calulations.[24,27] Although Gouterman's models were developed over 20 years ago, no subsequent theoretical calculations have been reported that account for the MCD spectral data of MPc(−2) complexes in a more satisfactory manner.[28]

Gouterman's model of the electronic structure has therefore been used as the theoretical framework within which to assign the $\pi \rightarrow \pi^*$ transitions of a variety of MPc(−2) and MP(−2) complexes and their cation and anion radicals to the bands calculated in spectral deconvolution studies based on UV−visible absorption and MCD spectroscopy,[29] by our research

(17) (a) Tse, Y. H.; Goel, A.; Hu, M.; Lever, A. B. P. ; Leznoff, C. C.; Van Lier, J. E. *Can. J. Chem.* **1993**, *71*, 742. (b) Fu, Y.; Forman, M.; Leznoff, C. C.; Lever, A. B. P. *J. Phys. Chem.* **1994**, *98*, 8985. (c) McKeown, N. B.; Leznoff, C. C. *Mol. Cryst. Liq. Cryst.* **1992**, *213*, 91.
(18) Konami, H.; Ikeda, Y.; Hatano, M.; Mochizuki, K. *Mol. Phys.* **1993**, *80*, 153.
(19) Kobayashi, N. In *Phthalocyanine. Principles and Properties*; Leznoff, C. C., Lever, A. B. P., Eds.; VCH Publications: New York, 1989; Vol. 2, Chapter 3, pp 97−163.
(20) Makorova, E. A.; Kopranenkov, V. N.; Shevtsov, V. K.; Luk'yanets, E. A. *Chem. Heterocycl. Compd. (Engl. Transl.)* **1989**, *10*, 1385.
(21) Leznoff, C. C.; McKeown, N. B. *J. Org. Chem.* **1990**, *55*, 2186.
(22) (a) Gouterman, M. In *The Porphyrins*; Dolphin, D., Ed.; Academic Press: New York, 1978; Vol. III, Part A, pp 1−165. (b) Gouterman, M. *J. Mol. Spectrosc.* **1972**, *44*, 37. (c) Gouterman, M.; Wagniere, G. H.; Snyder, L. C. *J. Mol. Spectrosc.* **1963**, *11*, 108.
(23) (a) Michl, J. *J. Am. Chem. Soc.* **1978**, *100*, 6801. (b) Michl, J. *Pure Appl. Chem.* **1980**, *52*, 1549.
(24) Weiss, C.; Kobayashi, H.; Gouterman, M. *J. Mol. Spectrosc.* **1965**, *16*, 415.
(25) McHugh, A. J.; Gouterman, M.; Weiss, C. *Theor. Chim. Acta* **1972**, *24*, 346.
(26) Nyokong, T.; Gasyna, Z.; Stillman, M. J. *Inorg. Chem.* **1987**, *26*, 1087.
(27) Schaffer, A. M.; Gouterman, M.; Davidson, E. R. *Theor. Chim. Acta* **1973**, *30*, 9.
(28) (a) Henriksson, A.; Roos, B.; Sundbom, M. *Theor. Chim. Acta* **1972**, *27*, 303. (b) Dedieu, A.; Rohmer, M.-M.; Veillard, A. *Adv. Quantum. Chem.* **1982**, *16*, 43. (c) Orti, E.; Bredas, J. L.; Clarisse, C. *J. Chem. Phys.* **1990**, *92*, 1228. (d) Liang, X. L.; Flores, S.; Ellis, D. E.; Hoffman, B. M.; Musselman, R. L. *J. Chem. Phys.* **1991**, *95*, 403. (e) Rosa, A.; Baerends, E. J. *Inorg. Chem.* **1992**, *31*, 4717. (f) Rosa, A.; Baerends, E. J. *Inorg. Chem.* **1994**, *33*, 584. (g) Ishikawa, N.; Ohno, O.; Kaizu, Y.; Kobayashi, H. *J. Phys. Chem.* **1992**, *96*, 8832. (h) Ishikawa, N.; Ohno, O.; Kaizu, Y. *J. Phys. Chem.* **1993**, *97*, 1004.

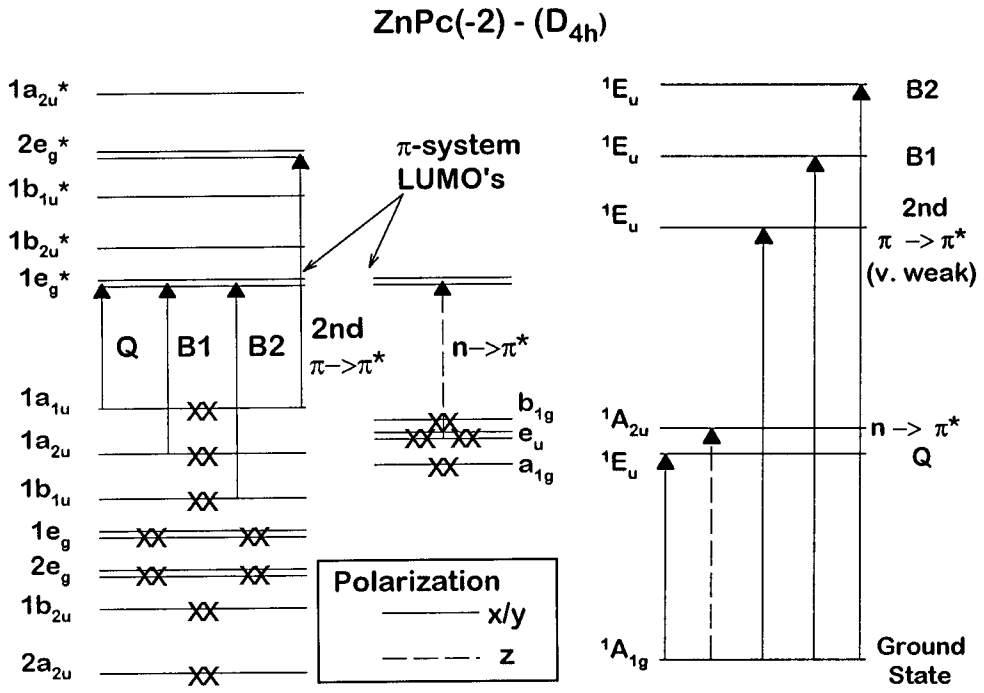

Figure 3. Molecular orbital (left) and state level (right) diagrams of MPc(−2) showing the one-electron transitions that are predicted to give rise to absorption bands in the 280−1000 nm range. The orbital ordering on the left is based on Gouterman's model of the inner ring cyclic polyene.[22] The orbitals on the right are the four aza nitrogen lone pair orbitals. The association of orbital angular momentum (OAM) with pairs of orbitals follows from the assignment of the molecular orbitals of the aromatic inner ring in terms of the OAM associated with the complex wave functions. Gouterman's original SCMO−PPP−CI model[24] contained five transitions labeled Q, B, N, L, and C. An additional B2 transition has been identified through spectral deconvolution studies of MPc species.[21,26,27,31−34,38] Transitions that give rise to *x/y*-polarized bands are represented with solid lines. Dashed lines are used for *z*-polarized transitions. The n → π^* transition is placed between the Q and B1 transitions on the basis of a spectral deconvolution analysis of (CN)ZnPc(−2).[38]

group using the program SIMPFIT.[3a,30−35] Spectral deconvolution of absorption and MCD spectra indicated that there are six intense *A* terms in the 250−700 nm region of main group MPc(−2) complexes. Gouterman assigned the major MP(−2) spectral bands to five major transitions labeled Q, B, N, L, and C (Figure 3). As the 300−450 nm region of MPc(−2) spectra contains two overlapping *A* terms the assignment scheme was modified to include separate B1 and B2 transitions.[3a,31] Recent MO calculations using the ZINDO program[36,37] have suggested that there is an additional weaker second $\pi \rightarrow \pi^*$ transition slightly to the red of the B1 transition which corresponds to the one-electron transition labeled as the L transition in Gouterman's assignment scheme.[36] Keeping the original labels,[3a,24,27] the higher energy N, L, and C bands were found to arise from a combination of a number of different one-electron transitions, but the original band nomenclature has been retained.[36,37]

The electronic structure of structurally modified phthalocyanine complexes has received considerably less attention than that of more highly symmetric MPc(−2) complexes. The spectral changes that result from the introduction of carbons to replace aza nitrogens have been known since the 1930s.[38] Savel'ev *et al.*[39] investigated the effect of the molecular structure of a number of phthalocyanine complexes including free base and Cu and Zn tetrabenzo[5]monoazaporphyrin (TBMAP) and free base TBTrAP on the spectroscopic properties of these complexes. Sevchenko *et al.*[40] have reported low-temperature polarization spectra of H_2TBTrAP and MgTBTrAP, and Solov'ev *et al.*[41] have analyzed the absorption spectra of various aza substituted tetrabenzporphyrins using a group theoretical approach. In 1975, Kolto *et al.*[42] investigated the fluorescence properties of a number of porphyrins and related molecules including ZnTBMAP. In recent years there has been renewed interest in the electrochemistry and optical spectroscopy of TBTrAP complexes.[17,19,21] In this paper, the optical spectroscopy of TBTrAP and TNTrAP is explored and molecular orbital

(29) The MCD signal arises from the same transitions as those seen in the UV−visible absorption spectrum, but the selection rules are different, as the intensity mechanism depends upon the magnetic dipole moment, in addition to the electric dipole moment, which normally determines UV−visible absorption intensity.[67] MCD spectroscopy is therefore complementary to UV−visible absorption spectroscopy, as it can provide ground and excited state degeneracy information essential in understanding the electronic structure of molecules of high symmetry. The specificity of the MCD technique arises from three highly characteristic spectral features, the Faraday *A*, *B*, and *C* terms.[67] The derivative-shaped Faraday A term is temperature independent and identifies degenerate excited states, while the normally Gaussian-shaped *C* term is highly temperature-dependent and identifies an orbitally degenerate ground state. Gaussian-shaped, temperature-independent *B* terms arise from mixing between closely related states linked by a magnetic dipole transition moment.

(30) Nyokong, T.; Gasyna, Z.; Stillman, M. J. *Inorg. Chem.* **1987**, *26*, 548.
(31) Ough, E. A.; Nyokong, T.; Creber, K. A. M.; Stillman, M. J. *Inorg. Chem.* **1988**, *27*, 2724.
(32) Ough, E. A.; Gasyna, Z.; Stillman, M. J. *Inorg. Chem.* **1991**, *30*, 2301.
(33) Gasyna, Z.; Stillman, M. J. *Inorg. Chem.* **1990**, *29*, 5101.
(34) Mack, J.; Stillman, M. J. *J. Am. Chem. Soc.* **1994**, *116*, 1292.
(35) Mack, J.; Stillman, M. J. *J. Phys. Chem.* **1995**, *99*, 7935.
(36) Cory, M. G.; Hirose, H.; Zerner, M. C. *Inorg. Chem.* **1995**, *34*, 2969.
(37) Mack, J.; Stillman, M. J. *Inorg. Chem.* **1997**, *36*, 413−425.
(38) (a) Barrett, P. A.; Linstead, R. P.; Tuey, G. A. P.; Robertson, J. M. *J. Chem. Soc.* **1939**, 1809. (b) Barrett, P. A.; Linstead, R. P.; Tuey, F. G.; Tuey, G. A. P. *J. Chem. Soc.* **1940**, 1079. (c) Dent, C. J. *J. Chem. Soc.* **1938**, 1. (d) Helberger, J. H. *Justus Liebigs Ann. Chem.* **1937**, *529*, 205.
(39) Savel'ev, D. A.; Kotlyar, I. P.; Sidorov, A. N. *Zh. Fiz. Khim.* **1969**, *43*, 1914; *Chem. Abstr.* **1970**, *72*, 11824j.
(40) Sevchenko, A. N.; Mashenkov, V. A.; Solov'ev, K. N. *Dokl. Akad. Nauk SSSR* **1968**, *179*, 61; *Chem. Abstr.* **1968**, *69*, 14559a.
(41) Solov'ev, K. N.; Mashenkov, V. A.; Kachura, T. F. *Opt. Spectrosc.* **1969**, *27*, 24.
(42) Kolto, V. N.; Solov'ev, K. N.; Shkirmam, S. F. *Izv. Akad. Nauk SSSR, Ser. Fiz.* **1975**, *39*, 1972; *Chem. Abstr.* **1976**, *84*, 23911w.

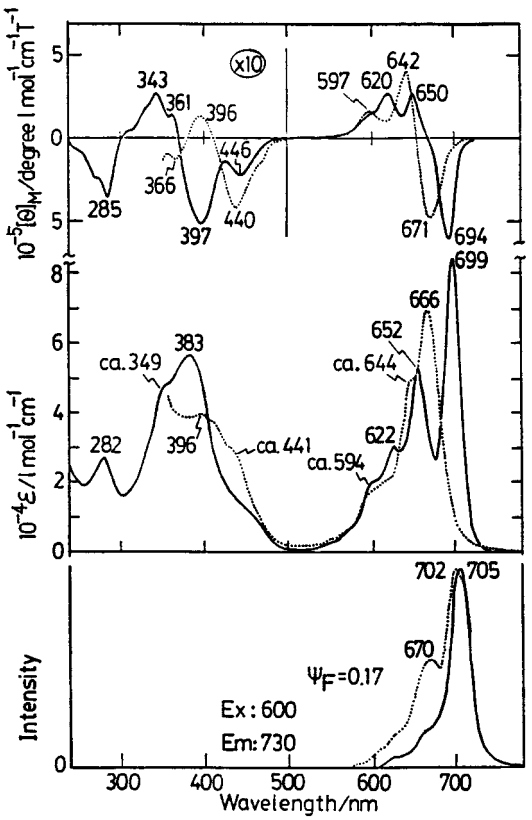

Figure 4. MCD (top), electronic absorption (middle), and fluorescence excitation spectra (bottom) of neutral (solid lines) and deprotonated (dotted lines) compound **A** in THF.

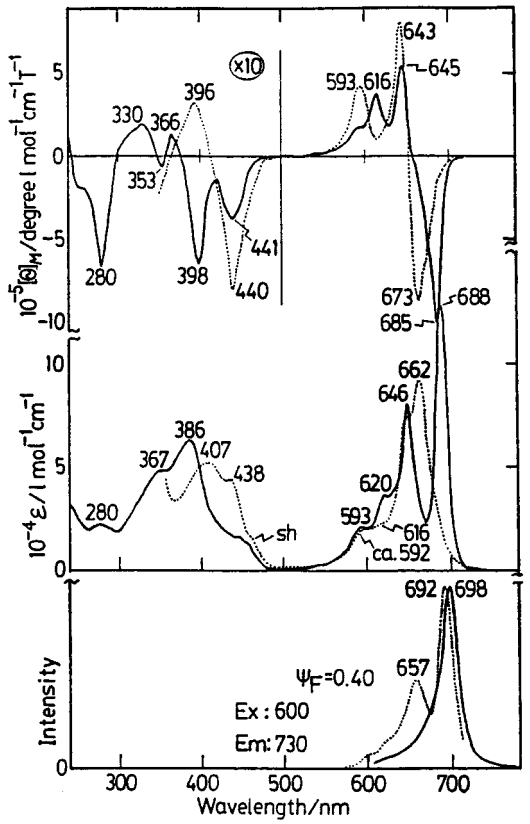

Figure 5. MCD (top), electronic absorption (middle), and fluorescence excitation spectra (bottom) of neutral (solid lines) and deprotonated (dotted lines) compound **B** in THF.

calculations are reported using the ZINDO program[43] to account for the bands observed. The recent study of Tse *et al.*[17a] has shown that, although the UV−visible spectra of neutral and cationic TBTrAP species appear to be similar to those of analogous phthalocyanine species, the spectra of the anion radical species are markedly different. MCD spectroscopy is used to investigate the electronic structure of TBTrAP and related complexes within the context of the models that have been developed to account for the spectroscopic properties of the phthalocyanines. The MCD spectrum of the anion radical of the TBTrAP ring is compared with those reported for phthalocyanine π-anion radicals.[3b,34,44]

Experimental Section

The synthesis of the complexes studied has been reported elsewhere.[17a,21] The UV−visible absorption, fluorescence, and magnetic circular dichroism spectra reported in Figures 4−6 were recorded with a Shimadzu UV-250 spectrometer, and the magnetic circular dichroism (MCD) measurements were made with a JASCO J-500 spectropolarimeter equipped with a JASCO electromagnet with a field strength of 1.53 T. The solvents used to measure the absorption and MCD spectra in Figures 4−6 were methylene chloride for the deprotonated complexes and THF for the free base complexes. Deprotonation was carried out by adding an aliquot of concentrated tetrabutylammonium hydroxide.[45] The fluorescence and excitation spectra were recorded with a Shimadzu RF-500 spectrofluorimeter. The absorbance at the excitation wavelengths was always less than 0.05. Fluorescence quantum yields were determined through comparative calibration using H_2Pc ($\Phi_F = 0.60$) and ZnPc ($\Phi_F = 0.30$) in 1-chloronaphthalene[46] or *tert*-butylated tetrabenzporphyrin ($\Phi_F = 0.30$) in chloroform.[47] Fluorescence decay curves were obtained at 20 °C with a Horiba NAES series instrument using glass filters and a monochromator to monitor the emission. All sample solutions for fluorescence measurements were purged with argon. The fluorescence experiments were carried out at concentrations as low as 10^{-7} M, where aggregation phenomena may be neglected.

The ring-reduced anion radical species of tetraneopentoxyphthalocyanine (TNPc) and TBTrAP were prepared photochemically using hydrazine in a DMF/hydrazine hydrate solvent mixture.[34] The addition of excess hydrazine hydrate to a solution of free base phthalocyanine results in the formation of a complex in which two protonated solvent molecules are believed to assume an axial coordination that results in a higher molecular symmetry.[48,49] Anion radical species are generated through selective wavelength irradiation with a 300 W tungsten−halogen Kodak projector lamp and a Corning CS 2-73 filter under a nitrogen atmosphere. Hydrazine acts as the electron donor.[34] The absorption spectra of the anion radical species were recorded with an Aviv 17 DS spectrometer (a modified Cary 17 spectrometer) and are almost identical to those obtained previously by Tse *et al.*[17] following electrochemical reduction. The anion radical MCD spectra shown in Figure 7 were recorded with a JASCO J-500C spectropolarimeter and an Oxford Instruments SM2 superconducting magnet (5.6 T field strength) under the control of an upgraded version of the program CDSCAN[50,51] running on an IBM 9000 series computer. The field strength and sign were calibrated by measuring the MCD spectrum of an aqueous solution of $CoSO_4$ at 510 nm. $[\theta]_M$ was calculated for this instrument to be -59.3 deg·cm^2·dmol^{-1}·T^{-1}. The signal intensity of the CD spectrometer was also tested using ammonium *d*-camphor-10-

(43) CAChe Scientific, P.O. Box 500, Mail Station 13-400, Beaverton, OR 97077.
(44) Mack, J.; Kirkby, S.; Ough, E. A.; Stillman, M. J. *Inorg. Chem.* **1992**, *31*, 1717.
(45) Dodworth, E. S.; Lever, A. B. P.; Seymour, P.; Leznoff, C. C. *J. Phys. Chem.* **1985**, *89*, 5698.
(46) Seybold, P. G.; Gouterman, M. *J. Mol. Spectrosc.* **1971**, *39*, 421.
(47) Kobayashi, N.; Numao, M.; Kondo, R.; Nakajima, S.; Osa, T. *Inorg. Chem.* **1991**, *30*, 2241.
(48) Martin, K. A.; Stillman, M. J. *Can. J. Chem.* **1979**, *57*, 1111.
(49) Martin, K. A.; Stillman, M. J. *Inorg. Chem.* **1980**, *19*, 2473.
(50) Mack, J. Ph.D. Thesis, University of Western Ontario, 1994.
(51) Gasyna, Z.; Browett, W. R.; Nyokong, T.; Kitchenham, R.; Stillman, M. *J. Chemom. Intell. Lab. Syst.* **1989**, *5*, 233.

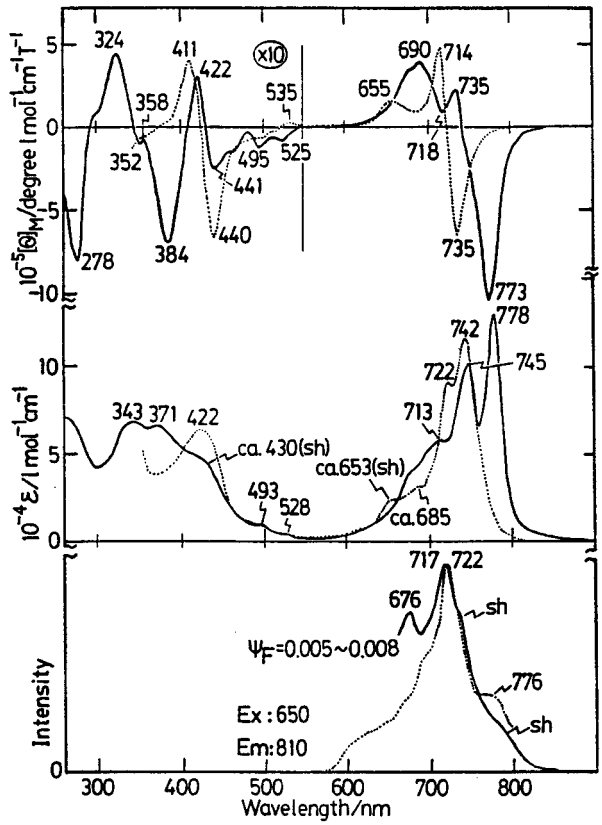

Figure 6. MCD (top), electronic absorption (middle), and fluorescence excitation spectra (bottom) of neutral (solid lines) and dianionic (dotted lines) compound **C** in THF.

sulfonate by ensuring that the θ^0/A ratio for the peaks at 280 nm was 2.26.[52] Baselines were subtracted using SPECTRA MANAGER.[53] Electron paramagnetic resonance (EPR) measurements were made on a Bruker Model ESR 300 X-band spectrometer, at 77 K in a liquid-nitrogen dewar. Solutions of ZnPc, H_2TNPc, and H_2TBTPAP each in a DMF/hydrazine hydrate solvent mixture (4:1) were siphoned into 2 mm i.d. quartz tubes, sealed under an inert gas atmosphere, irradiated, and quenched in liquid nitrogen. An external DPPH standard was used to calculate *g* factors.

Results

Absorption and MCD Spectroscopy. The absorption and MCD spectra of the free base (solid lines) and dianionic (dotted lines) species of compounds **A**−**C** are shown in Figures 4−6. The spectra of the free base species are similar to those that have been reported for H_2Pc.[3a] The lowest energy $\pi \rightarrow \pi^*$ transition gives rise to two major bands in the 650−800 nm region followed at higher energies by a complex envelope of vibrational bands. For the neutral **A**, band maxima are at 652 and 699 nm, for **B** at 646 and 688 nm, and for **C** at 742 and 778 nm. As the symmetries of the free base and dianionic species are C_s and C_{2v}(I), respectively, the MCD spectra exhibit only Faraday *B* terms.[54] The major lowest energy $\pi \rightarrow \pi^*$ bands overlap significantly in the absorption spectra but are resolved in the MCD spectra as separate negative and positive *B* terms. The 250−450 nm region of the spectrum is much more complex. In the spectra of the free base TBTrAP complexes, **A** and **B**, solid lines in Figures 4 and 5, a negative *B* term at 446 and 441 nm, respectively, is followed by a complex set of negative and positive *B* terms. These bands appear to red-shift significantly in the spectrum of dianionic TBTrAP complexes, dashed lines in Figures 4 and 5. The spectrum of the free base TNTrAP complex, **C**, solid line in Figure 6, contains weak negative *B* terms at 525 and 495 nm followed by more intense alternating negative and positive *B* terms to higher energy.

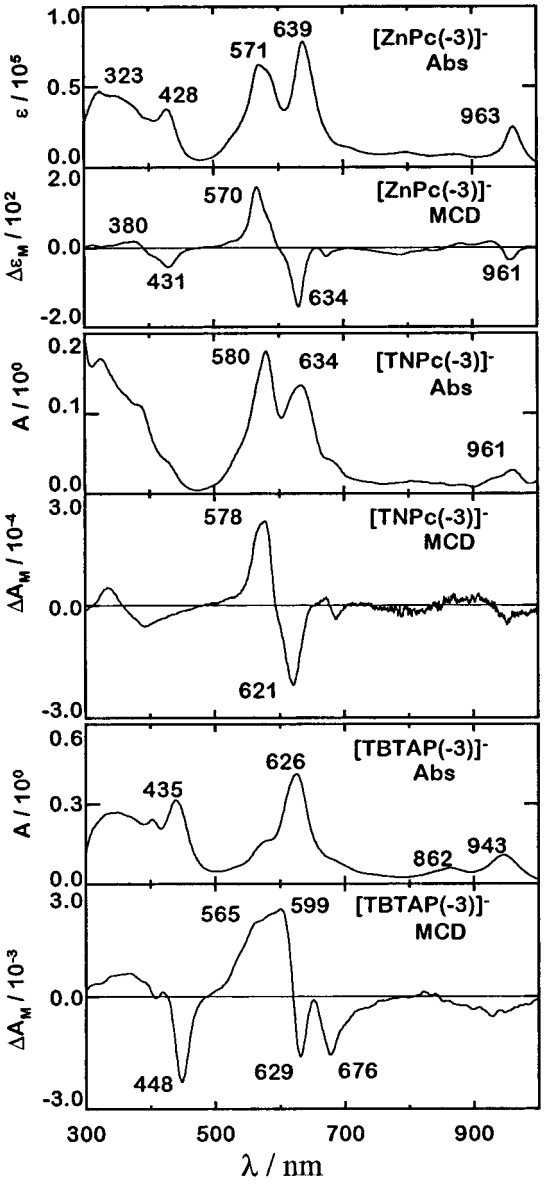

Figure 7. Absorption and MCD spectra of $[ZnPc(-3)]^-$, $[TNPc(-3)]^-$, and the dimeric $[TBTrAP(-3)]^-$ species of compound **B**.

The absorption and MCD spectra of TBTrAP(−3) appear to be very different from those of TNPc(−3) and $[ZnPc(-3)]^-$, Figure 7. The absorption spectra of $[ZnPc(-3)]^-$ and TNPc(−3) are dominated by a pair of well-resolved absorption bands in the 500−700 nm region. In contrast, the absorption spectrum of TBTrAP(−3) is dominated by a single intense band at 626 nm. An intense pair of oppositely signed *B* terms dominate

(52) Chen, G. C.; Yang, J. T. *Anal. Lett.* **1977**, *10*, 1195.
(53) Browett, W. R.; Stillman, M. *J. Comput. Chem.* **1987**, *11*, 73.

(54) The ground states of divalent, main group D_{4h} MPc(−2) complexes are $^1A_{1g}$, and the accessible $\pi \rightarrow \pi^*$ excited states will be degenerate, ^1E_u (*x*/*y* polarization), Figure 3. The major $\pi \rightarrow \pi^*$ transitions which dominate the UV−visible region of the optical spectra of MPc(−2) complexes give rise to Faraday *A* terms in the MCD spectra. Vibronically coupled and $n \rightarrow \pi^*$ states can also transform as $^1A_{2u}$ (*z* polarization), giving rise to Faraday *B* terms. The ground state of H_2Pc is ^1A_g, and the accessible $\pi \rightarrow \pi^*$ excited states will be $^1B_{3u}$ and $^1B_{2u}$ (with *x* and *y* polarization). As a result, the major $\pi \rightarrow \pi^*$ transitions which dominate the UV−visible region of the optical spectra of H_2Pc and other complexes with symmetry lower than D_{4h} give rise to oppositely signed coupled *B* terms rather than *A* terms in the MCD spectra.

the $[ZnPc(-3)]^-$ MCD spectrum at 571 and 635 nm and also the TNPc(−3) spectrum at 566 and 626 nm. Again, in contrast, the MCD spectrum of TBTrAP(−3), Figure 7, in the 500−700 nm region contains a pair of intense negative *B* terms followed by an envelope of overlapping positive *B* terms. The 700−1000 nm region of the TBTrAP(−3) absorption spectrum contains an envelope of overlapping bands with λ_{max} values at 943 and 862 nm that superficially appear to be very similar to those of the spectra of TNPc(−3) and $[ZnPc(-3)]^-$. The MCD spectra are clearly very different, however. The MCD spectrum of TBTrAP(−3) contains a broad envelope of negative *B* terms in the 800−1000 nm region. In contrast, the spectra of $[ZnPc(-3)]^-$ and TNPc(−3) contain a more complex set of both negative and positive *B* terms, Figure 7. The absorption spectrum of TBTrAP(−3) is reasonably similar to that of $[ZnPc(-3)]^-$ in the 300−500 nm region. The negative *B* term at 448 nm in the TBTrAP(−3) spectrum is, however, significantly more intense than the corresponding band in the $[ZnPc(-3)]^-$ spectrum and lies significantly to the blue of the intense absorption band at 435 nm, Figure 7. The corresponding band is significantly less intense in the spectrum of TNPc(−3) and appears as a shoulder in the absorption spectrum and as a weak *B* term in the MCD spectrum near 430 nm. The MCD spectra of TBTrAP(−3), TNPc(−3), and $[ZnPc(-3)]^-$ each contain negative *B* terms in the 420−460 nm region that are followed to high energy by overlapping positive *B* terms.

Emission Spectroscopy. The S1 fluorescence excitation spectra of compounds **A**−**C** are shown at the bottom of Figures 4−6 together with their quantum yields (Ψ_F). In contrast to the case of TBMAP, no emission data have been reported for the TBTrAP complexes.[41] As was found previously, the Φ_F values of reduced-symmetry, partially aza substituted porphyrins are much smaller than those of the corresponding Pc complexes in the same solvents.[55−58] For example, free base tetra-*tert*-butylated phthalocyanine (*t*-Bu-H_2Pc) and naphthalocyanine (^{t}Bu-H_2NPc) have Φ_F values of 0.85 and 0.14, respectively,[57] as compared with values of 0.40 and 0.005−0.008 for complexes **B** and **C**. The emission lifetimes (τ) for compounds **A** and **B** (τ = ca. 5.4 ns) are similar to, but smaller than, those of H_2TNPc (7.3 ns)[58] and *t*-Bu-H_2Pc (7.2 ns)[57] and larger than the value of compound **C** (3.8 ns).

Molecular Orbital Calculations. The structures for our MO calculations were obtained through the use of a Tektronics Inc. CAChe workstation.[43] The peripheral substitution of complexes **A**−**C** was not included in the structures used to generate the MO calculations as it has little spectral impact.[3a] The structures were refined using a modified MM2 force field calculation in the Mechanics program of the CAChe system.[59] The structures were optimized at the restricted Hartree−Fock self-consistent field (SCF) level[60] in the case of the diamagnetic species and at the restricted open-shell Hartree−Fock (ROHF) SCF level[61] in the case of the paramagnetic species using the ZINDO program in the CAChe software package.[62] These SCF optimizations were carried out at the intermediate neglect of differential overlap/1[63] (INDO/1) level of approximation. The structures were then used to obtain calculated UV−visible absorption spectra using the spectroscopic INDO Hamiltonian (INDO/S),[62a,b] Tables 1−6 (see Supporting Information for Tables 5 and 6), for free base and dianionic Pc, TBTrAP, and TNTrAP. The active orbitals in the configuration interaction (CI) calculation were the 22 lowest energy unoccupied and 22 highest energy occupied molecular orbitals, Figures 8−11 (see Supporting Information for Figures 10 and 11). The dianionic species were calculated using Zn(II) as the central counterion. No significant metal to ligand or ligand to metal charge transfer was seen in the 250−1000 nm region for ZnPc(−2).

The calculation predicts that the Q and B1 bands of Pc(−2) will lie at 676 and 291 nm, Table 1, which is in good agreement with previous experimental results.[3a] The calculated energies of the frontier orbitals of the dianionic species of Pc, TBTrAP, tetrabenzo[5,15]diazaporphyrin (TBDAPo), tetrabenzo[5,10]-diazaporphyrin (TBDAPa), TBMAP, tetrabenzporphyrin (TBP), and TNTrAP are shown schematically in Figure 12. The energy levels show good agreement with the second reduction potential for free base TBTrAP, which is about 300 mV more negative than those of free base phthalocyanine, suggesting a wider energy gap between the HOMO and the LUMO.[17a] The redox results also indicated that free base H_2TNTrAP species are more easily oxidized than the analogous H_2TBTrAP complexes as the binding energy of the HOMO electrons is lower.[17a]

The impact of perturbations on the electronic structure of the ideal cyclic polyene running around the perimeter of the porphyrin π-system can be predicted qualitatively by considering the location of the nodes and antinodes of the four frontier orbitals.[18,22,23,41] The pyrrolic nitrogens of the porphyrin molecule lie on a node of the HOMO a_{2u} orbital and very close to the nodes of the second HOMO a_{1u} orbital. As a result, the impact on the separation between the two HOMO orbitals (ΔHOMO) in porphyrin molecules is very slight as these orbitals lie close enough in energy that they can be viewed as being essentially degenerate and the B and Q transitions retain their allowed and forbidden characters. The nodal and antinodal patterns of the porphyrin and phthalocyanine e_g LUMO differ only along the *x* and *y* axes so the degeneracy of these orbitals can only be lifted through an asymmetrical perturbation of the structure. The impact of aza substitution on the energies of the LUMO's is therefore minimal, Figure 12, as the bridging positions lie close to the antinodes of both orbitals.

The a_{1u} HOMO of Pc has a node at the bridging 5-, 10-, 15-, and 20-positions, while the a_{2u} second HOMO has an antinode at these same atoms so perturbations to the ideal cyclic polyene structure result in a significant lifting of the degeneracy of the HOMO's. As a result, the Q transition gains intensity to become the dominant feature of the optical spectrum.[3a] The energy of the HOMO orbital remains essentially fixed on going from Pc to TBP, Figure 12, as the nodes of the HOMO are located on

(55) Kobayashi, N.; Ashida, T.; Osa, T. *Chem. Lett.* **1992**, 1567, 2031.
(56) Kobayashi, N.; Ashida, T.; Osa, T.; Konami, H. *Inorg. Chem.* **1994**, *33*, 1735.
(57) Kobayashi, N.; Higashi, Y.; Osa, T. *Chem. Lett.* **1994**, 1813.
(58) Kobayashi, N.; Lam, H.; Nevin, W. A.; Janda, P.; Leznoff, C. C.; Koyama, T.; Monden, A.; Shirai, H. *J. Am. Chem. Soc.* **1994**, *116*, 879.
(59) Purvis, G. D., III. *Comput. Aided Mol. Des.* **1991**, *5*, 55.
(60) Roothaan, C. C. J. *Rev. Mod. Phys.* **1951**, *23*, 69.
(61) (a) McWeeny, R.; Diercksen, G. J. *Chem. Phys.* **1968**, *49*, 4852. (b) Guest, M. F.; Saunders, V. R. *Mol. Phys.* **1968**, *28*, 819. (c) Binkley, J. S.; Pople, J. A.; Dobosh, P. A. *Mol. Phys.* **1974**, *28*, 1423. (d) Davidson, E. R. *Chem. Phys. Lett.* **1973**, *21*, 565. (e) Faegri, K.; Manne, R. *Mol. Phys.* **1976**, *31*, 1037. (f) Hsu, H.; Davidson, E. R.; Pitzer, R. M. *J. Chem. Phys.* **1976**, *65*, 609.
(62) (a) Ridley, J. E.; Zerner, M. C. *Theor. Chim. Acta* **1973**, *32*, 111. (b) Zerner, M. C.; Loew, G. H.; Kirchner, R. F.; Mueller-Westerhoff, U. T. *J. Am. Chem. Soc.* **1980**, *102*, 589. (c) Ridley, J. E.; Zerner, M. C. *Theor. Chim. Acta* **1976**, *42*, 223. (d) Bacon, A.; Zerner, M. C. *Theor. Chim. Acta* **1979**, *53*, 21. (e) Head, J.; Zerner, M. C. *Chem. Phys. Lett.* **1985**, *122*, 264. (f) Head, J.; Zerner, M. C. *Chem. Phys. Lett.* **1986**, *131*, 359. (g) Anderson, W.; Edwards, W. D.; Zerner, M. C. *Inorg. Chem.* **1986**, *25*, 2728. (h) Edwards, W. D.; Zerner, M. C. *Theor. Chim. Acta* **1987**, *72*, 347. (i) Kotzian, M.; Roesch, N.; Zerner, M. C. *Theor. Chim. Acta* **1992**, *81*, 201. (j) Kotzian, M.; Roesch, N.; Zerner, M. C. *Int. J. Quantum Chem.* **1991**, 545.
(63) Pople, J. A.; Beveridge, D.; Dobash, P. A. *Chem. Phys.* **1967**, *47*, 2026.

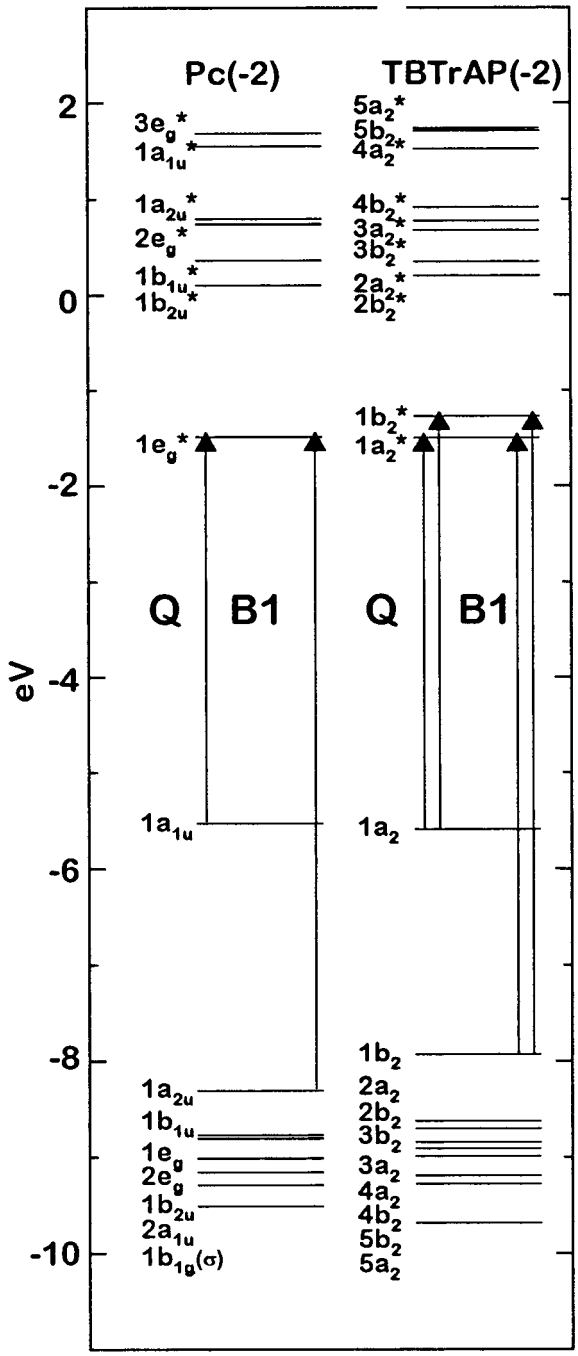

Figure 8. The 10 lowest energy unoccupied and 10 highest energy occupied molecular orbitals from the ZINDO calculation of $[Pc(-2)]^{2-}$ and $[TBTrAP(-2)]^{2-}$. The Q and B1 transitions refer to the two lowest energy $\pi \rightarrow \pi^*$ transitions into the LUMO. The MO labels are listed in ascending order adjacent to the orbital lines, which are plotted according to their calculated energies.

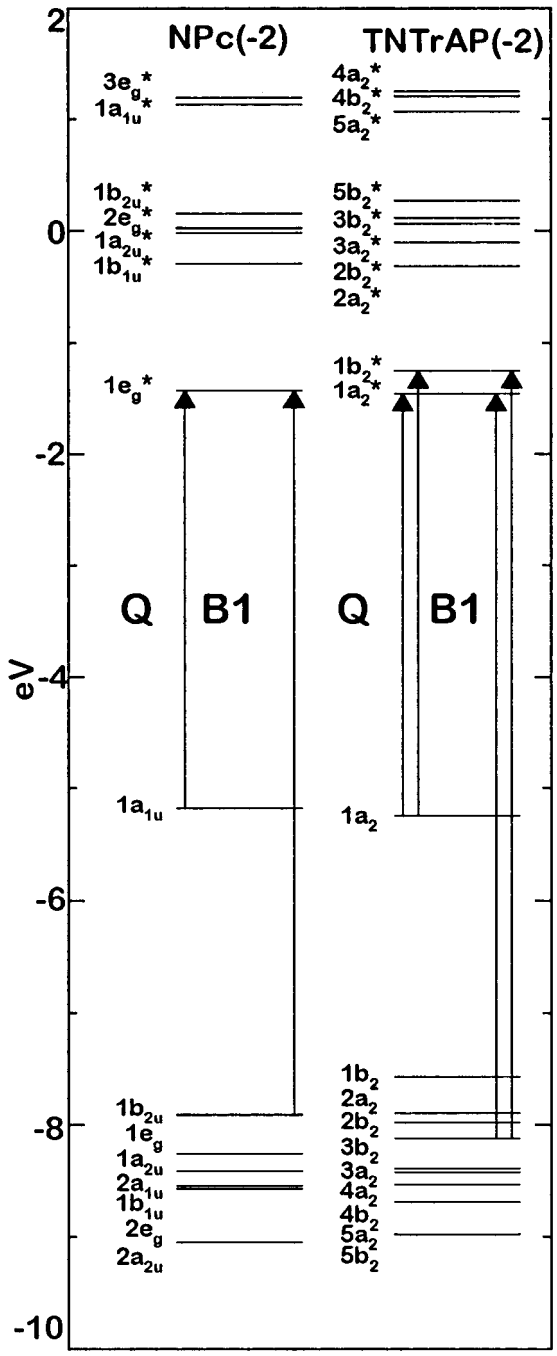

Figure 9. The 10 lowest energy unoccupied and 10 highest energy occupied molecular orbitals from the ZINDO calculation of $[NPc(-2)]^{2-}$ and $[TNTrAP(-2)]^{2-}$. The Q and B1 transitions refer to the two lowest energy $\pi \rightarrow \pi^*$ transitions into the LUMO and out of the highest energy occupied MO's associated with the inner perimeter of the ring. The MO labels are listed in ascending order adjacent to the orbital lines, which are plotted according to their calculated energies.

the bridging atoms at the 5-, 10-, 15-, and 20-positions. Aza substitution has a much greater impact on the energy of the second HOMO as the bridging positions lie close to the antinodes of the orbital. Therefore, the progressive addition of aza nitrogens on going from TBP to Pc results in a steady increase in ΔHOMO, Figure 12. The LUMO and HOMO's of TNTrAP have significantly different energies as the π-system of the ligand is expanded significantly through the addition of fused naphthalenes rather than fused benzenes to the periphery. The expansion of the π-system to form TNTrAP therefore results in a significant red shift of the Q band, Figures 4−6, and an increase in ratio between the Q band and B1 band intensities relative to that seen in the spectra of TBTrAP, Tables 1−6 (see Supporting Information for Tables 5 and 6), as has been noted previously for Pc and naphthalocyanine (NPc).[64]

Discussion

Assignment of the Optical Spectra of Free Base and Deprotonated TBTrAP and TNTrAP. Our MO calculations indicate that aza substitution at the bridging 5-, 10-, 15-, and 20-positions has a relatively minor impact on the energies of the major transitions, Figure 12. The assignment of the lowest

(64) Kobayashi, N.; Nakijima, S.; Osa, T. *Inorg. Chim. Acta* **1993,** *210*, 131.

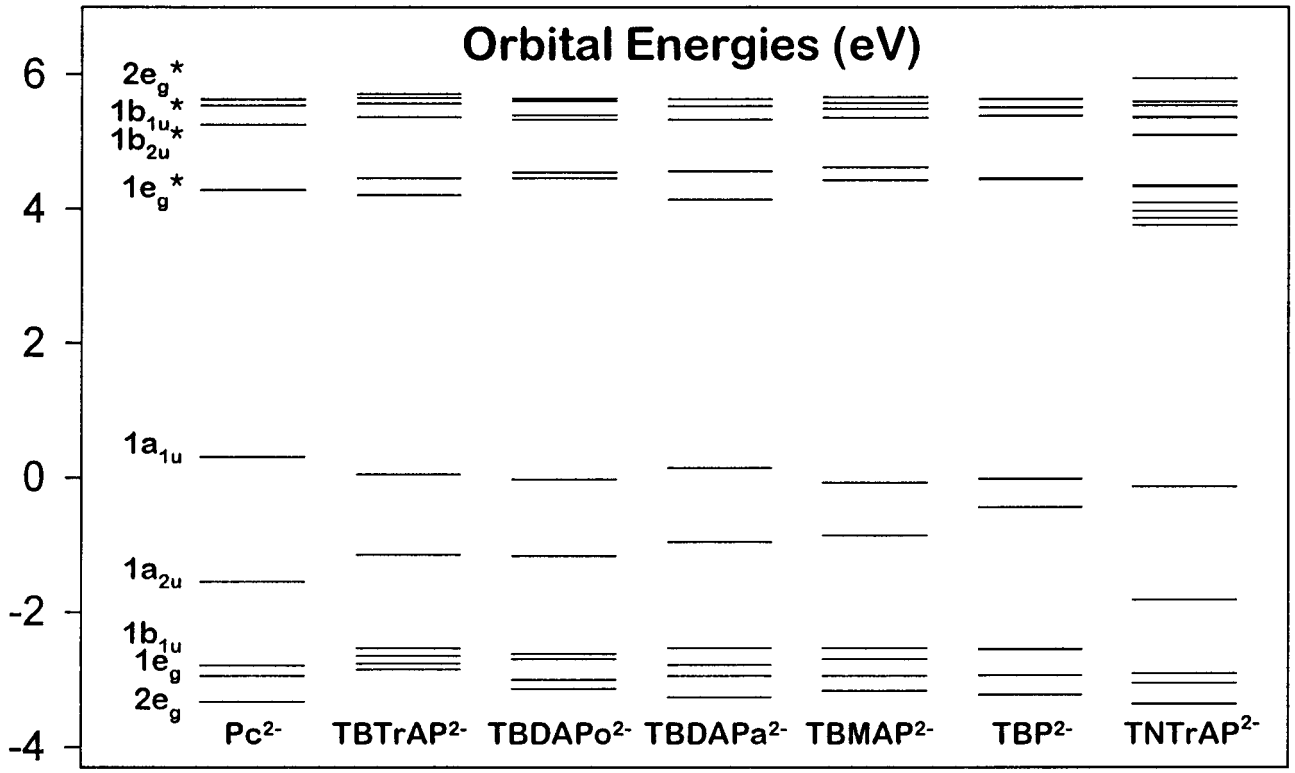

Figure 12. Partial molecular orbital energy diagram from the ZINDO calculations of $[Pc(-2)]^{2-}$, $[TBTrAP(-2)]^{2-}$, $[TBDAPo(-2)]^{2-}$, $[TBMAP(-2)]^{2-}$, $[TBP(-2)]^{2-}$ and $[TNTrAP(-2)]^{2-}$, showing the 6 highest occupied and 6 lowest unoccupied MO's of the first five complexes and the 6 highest occupied and 12 lowest unoccupied MO's of $[TNTrAP(-2)]^{2-}$.

Table 1. Calculated Electronic Excitations of $[Pc(-2)]^{2-}$

no.[a]	sym[b]	calcd[c]	obsd[d]	wave function[e]	assignment[f]
1	A_{1g}				ground state
2, 3	E_{ux}	14 780 (0.902)	14.8	$0.951\|1e_g^*\leftarrow 1a_{1u}\rangle + 0.260\|1e_g^*\leftarrow 1a_{1u}\rangle + ...$	Q
6, 7	E_{ux}	29 970 (0.019)		$-0.978\|2e_g^*\leftarrow 1a_{1u}\rangle + ...$	2nd $\pi \rightarrow \pi^*$
13	A_{2u}	34 100 (0.032)	16.5	$0.561\|1e_g^*\leftarrow e_u^N\rangle + 0.472\|1b_{2u}^*\leftarrow 1b_{1g}^N\rangle + ...$	n $\rightarrow \pi^*$
14, 15	E_{ux}	34 360 (0.770)	25.5	$0.754\|1e_g^*\leftarrow 1b_{1u}\rangle - 0.362\|1e_g^*\leftarrow 1a_{2u}\rangle + 0.409\|1e_g^*\leftarrow 2a_{2u}\rangle - 0.238\|1b_{2u}^*\leftarrow 1e_g\rangle + ...$	B1
16, 17	E_{ux}	34 710 (1.885)	29.9	$0.760\|1e_g^*\leftarrow 1a_{2u}\rangle - 0.385\|1e_g^*\leftarrow 1b_{1u}\rangle + 0.348\|3e_g^*\leftarrow 1a_{1u}\rangle + 0.207\|1e_g^*\leftarrow 1a_{1u}\rangle + ...$	B2

[a] The number of the state assigned in terms of ascending energy by the ZINDO calculation. Only states which result from allowed electronic transitions with a nonzero oscillator strength are included in the table. [b] The symmetry of the state under D_{4h} symmetry. [c] The calculated band energies (10^3 cm^{-1}) and oscillator strengths in parentheses. [d] Observed band energies from the data of Nyokong *et al.*[30] [e] The calculated wave functions based on the eigenvectors produced by the configuration interaction calculation of the ZINDO program. The energies of the molecular orbitals are shown in Figure 8. *N* denotes orbitals associated with the aza nitrogen lone pair orbitals. [f] The assignment is described in the text.

energy $\pi \rightarrow \pi^*$ bands of TBTrAP and TNTrAP, in the 600−800 nm range, to the Q transition is, therefore, straightforward, Tables 1−4. Sevchenko *et al.*[40] assigned the bands at 446 and 441 nm for the TBTrAP complexes **A** and **B** to a *y*-polarized n $\rightarrow \pi^*$ transition linking the nonbonding aza nitrogen lone pair orbitals and the π-system of the TBTrAP ring. The band was found to be polarized perpendicular to the *x*- and *z*-polarized components of the Q transition. Under the C_{2v}(III) symmetry of TBTrAP(−2) complexes, the major 2-fold axis lies within the plane of the ligand.[65] As a result, the *y* axis corresponds to the *z* axis of D_{4h} MPc(−2) complexes. A recent spectral deconvolution analysis of the low-temperature absorption and MCD spectra of ZnPc(−2) identified the presence of a *z*-polarized n $\rightarrow \pi^*$ transition at 604 nm within the vibrational envelope of the Q transition.[35] The ZINDO calculation appears to significantly overestimate the energies of these n $\rightarrow \pi^*$ transitions.[37] The weak negative *B* terms at 495 and 525 nm in the spectrum of the TNTrAP(−2) complex **C** may also arise from n $\rightarrow \pi^*$ transitions. Our ZINDO calculations suggest, however, that weak bands associated with transitions out of the LUMO into higher energy π^* orbitals are also present in this region of the spectra of NPc(−2) and TNTrAP(−2) species, Tables 3 and 4. The ZINDO calculation suggests that there are six empty π^* TNTrAP(−2) MO's in the same energy range as the two LUMO's of TBTrAP(−2), Figures 8, 9, and 12.

The intense, overlapped negative and positive *B* terms seen in the 250−450 nm regions of the MCD spectra of the TBTrAP complexes **A** and **B**, Figures 4 and 5, can be assigned primarily to the B1 and B2 transitions, Tables 1 and 2. Deconvolution studies of MPc(−2) complexes have identified several separate but overlapping electronic $\pi \rightarrow \pi^*$ transitions in this region.[3a,30−33,38] These transitions are most easily identified through the −ve/+ve sequence to high energy seen in the signs of the Faraday *B* terms that are associated with the *x*- and *y*-polarized components of each transition. As the π-system is significantly larger, the higher energy spectral bands of NPc(−2) and TNTrAP(−2), Tables 3 and 4, arise from combinations of one-electron transitions significantly different from those seen in the calculated spectra of Pc(−2) and TBTrAP(−2), Tables 1 and 2. The bands at 422 and 441 nm are assigned primarily to a transition out of the $1b_2$ orbital into the $1a_2^*$ and $1b_2^*$ LUMO's. The bands in the 300−400 nm region can be assigned

(65) Donini, J. C.; Hollebone, B. R.; Lever, A. B. P. *Prog. Inorg. Chem.* **1977**, *22*, 225.

Table 2. Calculated Electronic Excitations of $[TBTrAP(-2)]^{2-}$

no.[a]	sym[b]	calcd[c]	obsd[d]	wave function[e]	assignment[f]
1	A_1				ground state
2	A_1	15 050 (0.831)	14.5	$-0.951\|1a_2^*\leftarrow 1a_2\rangle + 0.254\|1b_2^*\leftarrow 1b_2\rangle + ...$	Q
3	B_1	15 380 (0.688)	15.5	$0.882\|1b_2^*\leftarrow 1a_2\rangle - 0.300\|2a_2^*\leftarrow 1b_2\rangle + ...$	Q
4	B_1	25 830 (0.028)		$0.964\|2b_2^*\leftarrow 1a_2\rangle + ...$	
5	A_1	27 250 (0.036)		$0.950\|2a_2^*\leftarrow 1a_2\rangle + ...$	
6	A_1	30 520 (0.002)		$0.926\|3a_2^*\leftarrow 1a_2\rangle - 0.228\|2a_2^*\leftarrow 1a_2\rangle + ...$	
7	B_1	30 620 (0.001)		$-0.745\|4b_2^*\leftarrow 1a_2\rangle + 0.603\|3b_2^*\leftarrow 1a_2\rangle + ...$	
8	B_1	31 090 (0.001)		$0.750\|3b_2^*\leftarrow 1a_2\rangle + 0.650\|4b_2^*\leftarrow 1b_2\rangle + ...$	
9	B_1	32 080 (2.470)	25.1	$0.883\|1a_2^*\leftarrow 1b_2\rangle - 0.295\|1b_2^*\leftarrow 1a_2\rangle + ...$	B1
10	A_1	33 240 (0.171)		$-0.820\|1a_2^*\leftarrow 1a_1^N\rangle + 0.259\|1b_2^*\leftarrow 1b_1^N\rangle + 0.260\|2b_2^*\leftarrow 2b_1^N\rangle - 0.244\|2b_2^*\leftarrow 1b_1^N\rangle + 0.233\|1b_2^*\leftarrow 1b_2\rangle + 0.221\|2b_2^*\leftarrow 1b_1^N\rangle + ...$	$n \rightarrow \pi^*$
11	A_1	33 260 (1.874)	27.3	$0.768\|1b_2^*\leftarrow 1b_2\rangle + 0.275\|1a_2^*\leftarrow 2a_2\rangle - 0.248\|1a_2^*\leftarrow 1a_1^N\rangle + 0.221\|1a_2^*\leftarrow 1a_2\rangle + ...$	B1
12	B_1	33 580 (0.086)		$0.594\|1a_2^*\leftarrow 2b_2\rangle + 0.425\|1b_2^*\leftarrow 3a_2\rangle - 0.398\|1a_2^*\leftarrow 5b_2\rangle + 0.267\|1a_2^*\leftarrow 3a_2\rangle + ...$	
13	A_1	33 630 (0.033)		$-0.743\|1a_2^*\leftarrow 3a_2\rangle - 0.314\|1b_2^*\leftarrow 2b_2\rangle + 0.247\|1b_2^*\leftarrow 5b_2\rangle + 0.221\|1a_2^*\leftarrow 2b_2\rangle - 0.213\|1b_2^*\leftarrow 1b_2\rangle + ...$	
14	B_2	33 810 (0.018)	22.7	$-0.669\|1a_2^*\leftarrow 1b_1^N\rangle - 0.532\|1b_2^*\leftarrow 1a_1^N\rangle + 0.221\|2b_2^*\leftarrow 1a_1^N\rangle + ...$	$n \rightarrow \pi^*$
15	A_1	34 980 (0.205)	28.3	$0.795\|1a_2^*\leftarrow 2a_2\rangle + 0.320\|1b_2^*\leftarrow 2b_2\rangle + 0.244\|1b_2^*\leftarrow 1b_2\rangle + 0.212\|2b_2^*\leftarrow 2b_2\rangle + ...$	B2
16	B_1	35 340 (0.026)	30.3	$0.815\|1b_2^*\leftarrow 2a_2\rangle + 0.243\|2b_2^*\leftarrow 2a_2\rangle + 0.202\|1a_2^*\leftarrow 5b_2\rangle + ...$	B2
17	A_1	35 470 (0.153)		$0.372\|1b_2^*\leftarrow 3b_2\rangle + 0.362\|4a_2^*\leftarrow 1a_2\rangle - 0.314\|1a_2^*\leftarrow 4a_2\rangle - 0.257\|1b_2^*\leftarrow 2b_2\rangle + ...$	

[a] The number of the state assigned in terms of ascending energy by the ZINDO calculation. Only states which result from allowed electronic transitions with a nonzero oscillator strength are included in the table. [b] The symmetry of the state under C_{2v}(III) symmetry. [c] The calculated band energies (10^3 cm^{-1}) and oscillator strengths in parentheses. [d] Observed band energies from the data reported in this paper. [e] The calculated wave functions based on the eigenvectors produced by the configuration interaction calculation of the ZINDO program. The energies of the molecular orbitals are shown in Figure 8. *N* denotes orbitals associated with the aza nitrogen lone pair orbitals. [f] The assignment is described in the text.

Table 3. Calculated Electronic Excitations of $[NPc(-2)]^{2-}$

no.[a]	sym[b]	calcd[c]	obsd[d]	wave function[e]	assignment[f]
1	A_{1g}				ground state
2, 3	E_{ux}	13 520 (1.223)	13.3	$0.960\|1e_g^*\leftarrow 1a_{1u}\rangle + ...$	Q
7, 8	E_{ux}	23 470 (0.056)		$-0.975\|2e_g^*\leftarrow 1a_{1u}\rangle + ...$	2nd $\pi \rightarrow \pi^*$
10, 11	E_{ux}	31 170 (0.300)		$-0.558\|1e_g^*\leftarrow 1b_{2u}\rangle - 0.486\|1e_g^*\leftarrow 1a_{1u}\rangle + 0.213\|1e_g^*\leftarrow 2a_{1u}\rangle + 0.202\|1b_{1u}^*\leftarrow 2e_g\rangle + ...$	B1
19, 20	E_{ux}	34 060 (3.104)	29.4	$0.734\|1e_g^*\leftarrow 1a_{2u}\rangle + 0.325\|1e_g^*\leftarrow 1b_{1u}\rangle + 0.256\|1b_{1u}^*\leftarrow 2e_g\rangle + 0.225\|1e_g^*\leftarrow 2a_{2u}\rangle + 0.207\|1a_{2u}^*\leftarrow 2e_g\rangle + ...$	B2
24 ,25	E_{ux}	35 160 (0.011)		$-0.645\|1e_g^*\leftarrow 1b_{1u}\rangle - 0.361\|1e_g^*\leftarrow 1a_{2u}\rangle - 0.345\|1e_g^*\leftarrow 2a_{1u}\rangle - 0.237\|1b_{2u}^*\leftarrow 2e_g\rangle - 0.210\|1e_g^*\leftarrow 1a_{2u}\rangle + ...$	

[a] The number of the state assigned in terms of ascending energy by the ZINDO calculation. Only states which result from allowed electronic transitions with a nonzero oscillator strength are included in the table. [b] The symmetry of the state under D_{4h} symmetry. [c] The calculated band energies (10^3 cm^{-1}) and oscillator strengths in parentheses. [d] Observed band energies of CoPc(−2) from the data of Kobayashi *et al.*[63] [e] The calculated wave functions based on the eigenvectors produced by the configuration interaction calculation of the ZINDO program. The energies of the molecular orbitals are shown in Figure 9. [f] The assignment is described in the text.

to three sets of overlapped coupled *B* terms, bands 13 and 19, 15 and 18, and 16 and 17, in Table 4. Bands 15 and 18 correspond most closely to the bands associated with the B1 transition in the absorption and MCD spectra of TBTrAP(−2). The nodal pattern of the $3b_2$ orbital of TNTrAP(−2), Figure 9, corresponds closely to that of the $1a_{2u}$ orbital of Pc(−2), Figure 8.

The spectra of the free base and deprotonated TBTrAP and TNTrAP species show some minor differences, Figures 4−6. The splittings of the oppositely-signed *B* terms associated with the Q transitions are, however, considerably smaller in the case of the deprotonated spectra as these species are only subject to the distortion caused by the partial aza substitution at the bridging 5-, 10-, 15-, and 20-positions, Figures 4−6. The calculated spectra of H_2TBTrAP and H_2TNTrAP, Tables 5 and 6 (see Supporting Information), are considerably more complex than those of TBTrAP(−2) and TNTrAP(−2), Tables 2 and 4, as the molecular symmetry is lowered from D_{4h} to C_s.

Spectra of π-Anion Radical Species. As the absorption and MCD spectra of the anion radical species of the TBTrAP complex **B** are markedly different from those reported previously for $[MPc(-3)]^-$,[3b,34,44] the assignment of the spectral bands in Figure 7 is more difficult. The anion radical spectrum of complex **B** is typical of that seen for other TBTrAP(−3) species.[17a] Detailed deconvolution studies[34] of the low-temperature absorption and MCD spectra of $[ZnPc(-3)]^-$ and a MO calculation using the ZINDO program[37] suggest that when an electron is added to the π-system, static Jahn−Teller distortion reduces the molecular symmetry to no higher than C_{2v}(III). The spectral bands have been assigned to three sets of overlapping bands arising from the major transitions of the π-system, Figure 7. The two bands in the 500−700 nm region are assigned to a $\pi^* \rightarrow \pi^*$ transition out of the partially-occupied, Jahn−Teller split LUMO $\Delta M_L = \pm 5$ orbitals into the empty symmetrically-split $\Delta M_L = \pm 6$ orbitals in the cyclic polyene model of the electronic structure.[22] The more complex bands in the 700−1000 and 300−500 nm regions are assigned to Q and to overlapping B1 and B2 transitions into the partially occupied π^* LUMO orbital, respectively, Figure 13.

The absorption and MCD spectra of the anion radical of the peripherally substituted phthalocyanine complex, TNPc, are very similar to those of $[ZnPc(-3)]^-$. Typical derivative-shaped EPR signals were seen at $g = 2.0031 \pm 0.0004$ for $[ZnPc(-3)]^-$ and $g = 2.0031 \pm 0.0004$ for TNPc(−3). The presence of the EPR signals confirms the doublet spin multiplicity and the lack of dimerization. A direct comparison can therefore be made between the spectrum of the anion radical generated from the free base TNPc complex and the spectrum of $[ZnPc(-3)]^-$. The three sets of intense bands that comprise the spectrum of TNPc(−3) can be assigned to the same transitions as in $[ZnPc(-3)]^-$.[48] In contrast, no EPR signal was seen for the TBTrAP(−3) species. It can therefore be concluded that dimerization leads to a singlet ground state, as has been observed previously with many phthalocyanine cation radical species.[3b,32]

Table 4. Calculated Electronic Excitations of $[TNTrAP(-2)]^{2-}$

no.[a]	sym[b]	calcd[c]	obsd[d]	wave function[e]	assignment[f]
1	A_1				ground state
2	A_1	13 680 (1.126)	12.9	$0.961\|1a_2^*\leftarrow 1a_2\rangle + ...$	Q
3	B_1	14 080 (0.988)	13.4	$-0.950\|1b_2^*\leftarrow 1a_2\rangle + ...$	Q
4	A_1	21 250 (0.040)		$-0.937\|2a_2^*\leftarrow 1a_2\rangle + 0.276\|3a_2^*\leftarrow 1a_2\rangle + ...$	
5	B_1	23 830 (0.001)		$-0.824\|3b_2^*\leftarrow 1a_2\rangle - 0.513\|3b_2^*\leftarrow 1a_2\rangle + ...$	
6	A_1	24 070 (0.034)		$-0.927\|3a_2^*\leftarrow 1a_2\rangle - 0.272\|2a_2^*\leftarrow 1a_2\rangle + ...$	
7	B_1	24 100 (0.001)		$-0.807\|2b_2^*\leftarrow 1a_2\rangle + 0.494\|3b_2^*\leftarrow 1a_2\rangle - 0.216\|4b_2^*\leftarrow 1a_2\rangle + ...$	
8	B_1	24 340 (0.095)		$0.932\|4b_2^*\leftarrow 1a_2\rangle + ...$	
9	B_1	30 140 (1.199)	22.7	$-0.862\|1a_2^*\leftarrow 1b_2\rangle - 0.231\|5b_2^*\leftarrow 1a_2\rangle + ...$	
10	A_1	30 510 (0.445)	23.7	$0.477\|1b_2^*\leftarrow 1b_2\rangle - 0.425\|1a_2^*\leftarrow 3a_2\rangle + 0.266\|4a_2^*\leftarrow 1a_2\rangle + ...$	
11	B_1	30 980 (0.169)		$-0.602\|1a_2^*\leftarrow 2b_2\rangle + 0.448\|1a_2^*\leftarrow 3b_2\rangle + 0.266\|5b_2^*\leftarrow 1a_2\rangle - 0.206\|2b_2^*\leftarrow 5a_2\rangle + ...$	
12	A_1	31 540 (0.038)		$0.429\|5a_2^*\leftarrow 1a_2\rangle + 0.369\|1b_2^*\leftarrow 2b_2\rangle - 0.312\|1b_2^*\leftarrow 1b_2\rangle + 0.312\|1a_2^*\leftarrow 3a_2\rangle + ...$	
13	A_1	32 460 (0.634)		$-0.622\|1b_2^*\leftarrow 1b_2\rangle - 0.388\|5a_2^*\leftarrow 1a_2\rangle - 0.384\|1a_2^*\leftarrow 2a_2\rangle - 0.291\|6a_2^*\leftarrow 1a_2\rangle + 0.264\|1b_2^*\leftarrow 4b_2\rangle + ...$	
14	B_1	32 570 (0.051)		$-0.592\|1b_2^*\leftarrow 2a_2\rangle + 0.419\|5b_2^*\leftarrow 1a_2\rangle - 0.225\|1a_2^*\leftarrow 1b_2\rangle - 0.215\|3b_2^*\leftarrow 4a_2\rangle + ...$	
15	B_1	32 870 (2.012)	26.0	$-0.684\|1a_2^*\leftarrow 3b_2\rangle + 0.311\|1a_2^*\leftarrow 2a_2\rangle - 0.227\|1a_2^*\leftarrow 2b_2\rangle + 0.211\|2a_2^*\leftarrow 4b_2\rangle + ...$	"B1"
16	A_1	33 400 (0.814)		$0.507\|4a_2^*\leftarrow 1a_2\rangle - 0.424\|1a_2^*\leftarrow 5a_2\rangle + 0.408\|1a_2^*\leftarrow 2a_2\rangle - 0.295\|5a_2^*\leftarrow 1a_2\rangle - 0.285\|1b_2^*\leftarrow 3b_2\rangle + ...$	
17	B_1	34 040 (0.750)		$-0.534\|5b_2^*\leftarrow 1a_2\rangle - 0.449\|1a_2^*\leftarrow 2b_2\rangle + 0.331\|1b_2^*\leftarrow 2a_2\rangle - 0.222\|4a_2^*\leftarrow 1a_2\rangle + ...$	
18	A_1	34 050 (0.750)	30.9	$0.479\|4a_2^*\leftarrow 1a_2\rangle + 0.459\|1b_2^*\leftarrow 3b_2\rangle - 0.336\|6a_2^*\leftarrow 1a_2\rangle - 0.236\|5b_2^*\leftarrow 1a_2\rangle + 0.222\|1a_2^*\leftarrow 2a_2\rangle + ...$	"B1"
19	A_1	34 270 (0.326)		$-0.504\|1b_2^*\leftarrow 1b_2\rangle - 0.427\|6a_2^*\leftarrow 1a_2\rangle + 0.396\|5a_2^*\leftarrow 1a_2\rangle - 0.282\|1b_2^*\leftarrow 3b_2\rangle - 0.230\|4a_2^*\leftarrow 1a_2\rangle - 0.221\|2a_2^*\leftarrow 2a_2\rangle + 0.213\|8a_2^*\leftarrow 1a_2\rangle + ...$	
20	A_1	34 560 (0.008)		$-0.573\|6a_2^*\leftarrow 1a_2\rangle - 0.413\|1a_2^*\leftarrow 5a_2\rangle - 0.338\|4a_2^*\leftarrow 1a_2\rangle + 0.287\|1b_2^*\leftarrow 2b_2\rangle - 0.206\|7a_2^*\leftarrow 1a_2\rangle + ...$	

[a] The number of the state assigned in terms of ascending energy by the ZINDO calculation. Only states which result from allowed electronic transitions with a nonzero oscillator strength are included in the table. [b] The symmetry of the state under C_{2v}(III) symmetry. [c] The calculated band energies (10^3 cm^{-1}) and oscillator strengths in parentheses. [d] Observed band energies from the data reported in this paper. [e] The calculated wave functions based on the eigenvectors produced by the configuration interaction calculation of the ZINDO program. The energies of the molecular orbitals are shown in Figure 9. [f] The assignment is described in the text.

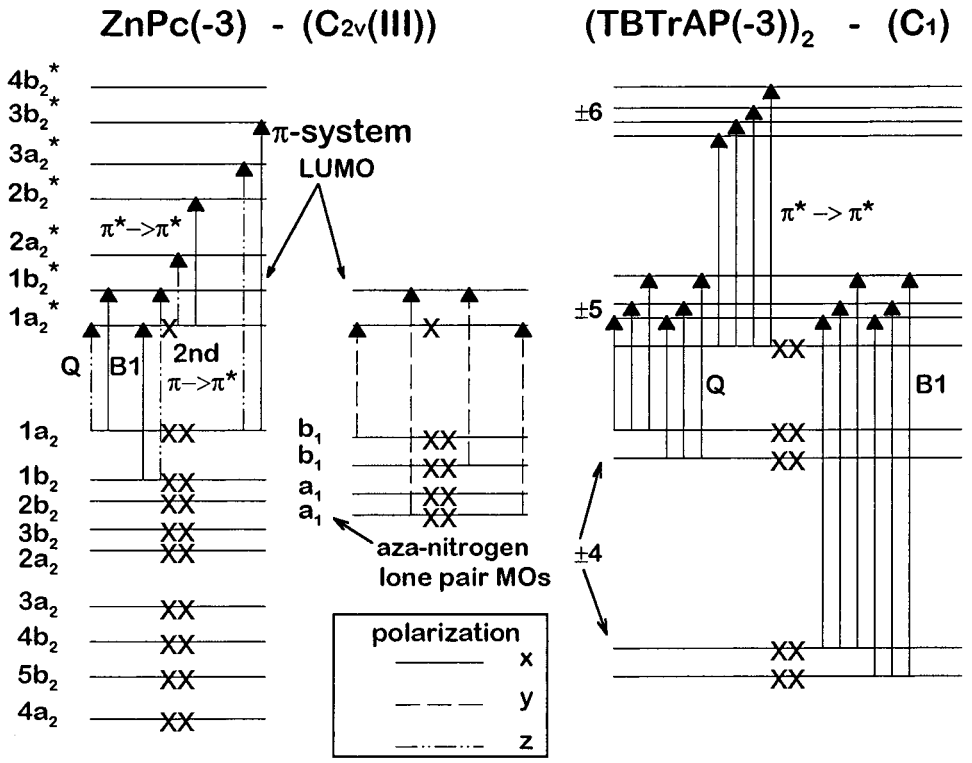

Figure 13. Molecular orbitals involved in the major $\pi \rightarrow \pi^*$ and $\pi^* \rightarrow \pi^*$ absorption transitions in the ring-reduced $[ZnPc(-3)]^-$ and the dimeric $[TBTrAP(-3)]^-$ species with energies between 10 000 and 35 000 cm^{-1}. The order of the orbitals is based on Gouterman's models of the electronic structure of porphyrin and phthalocyanine complexes.[22,24,25,28] The possible $\Delta M_L = \pm 1$ transitions are shown based on the application of Gouterman's 4-orbital LCAO model.[22] In addition to the $\pi \rightarrow \pi^*$ Q, B1, and B2 transitions of MPc(−2), Figure 3, there is a $\pi^* \rightarrow \pi^*$ transition out of the partially filled $\Delta M_L = \pm 5$ orbitals. The $[ZnPc(-3)]^-$ orbitals are labeled for C_{2v} geometry that results from the static Jahn−Teller distortion of the ring following reduction.[35] The symmetry of the dimeric $[TBTrAP(-3)]^-$ species is not expected to be higher than C_1.

Our ZINDO calculation of the major optical transitions of the π-system of free base and dianionic TBTrAP complexes has shown that the replacement of one of the aza nitrogens at the bridging positions does not have a major impact on the relative energies of the major $\pi \rightarrow \pi^*$ transitions, Tables 2 and 5. The transitions that dominate the spectra of TNPc(−3) and $[ZnPc(-3)]^-$ can therefore be expected to be responsible for the major bands seen in the B1/B2, $\pi^* \rightarrow \pi^*$, and Q spectral regions of TBTrAP(−3) between 300 and 500 nm, 500 and 700 nm, and 700 and 1000 nm, respectively. The complex series

of positive and negative *B* terms seen in the Q regions of the MCD spectra of both $[ZnPc(-3)]^-$ and TNPc(−3) is not seen in the case of TBTrAP(−3). We suggest that the explanation lies in the dimerization of the compound following photoreduction. As the ground state of the dimerized TBTrAP(−3) species no longer contains a partially filled LUMO orbital, the set of electronic configurations associated with the Q transition will be significantly different from those seen for the Q transition of the $[ZnPc(-3)]^-$ and TNPc(−3). The intensity mechanism for MCD *B* terms depends upon field-induced mixing of close-lying states linked by a magnetic dipole transition moment. An increased splitting of the LUMO due to dimerization would result in a greater separation between the excited states associated with the Q transition and a greatly reduced intensity for the bands associated with the Q transition in the MCD spectrum.

In the 500−700 nm region, the major peak in the absorption spectrum at 626 nm clearly arises from overlapping bands as there are both negative and positive *B* terms at 629 and 599 nm in the MCD spectrum. There appear to be two sets of overlapping positive and negative *B* terms in the MCD spectrum. Negative *B* terms at 676 and 629 nm are followed to high energy by positive *B* terms at 599 and 565 nm. All these bands can all be assigned to the $\pi^* \rightarrow \pi^*$ transition, as a second set of oppositely signed *B* terms is anticipated for a dimerized species, Figure 13. A static Jahn−Teller distortion of the π-system of the TBTrAP(−3) ring, similar to that of $[ZnPc(-3)]^-$, would reduce the molecular symmetry from C_{2v} to no higher than C_2 in the case of a monomeric species and probably to C_1 in the case of the TBTrAP(−3) dimer.

In the 300−500 nm region, the absorption spectrum of TBTrAP(−3) appears to be very similar to that of $[ZnPc(-3)]^-$ but the MCD spectrum is markedly different. The negative *B* term at 448 nm is more intense relative to the $\pi^* \rightarrow \pi^*$ bands than the corresponding bands in the spectra of TNPc(−3) and $[ZnPc(-3)]^-$ and lies well to the blue of the corresponding absorption band. The MCD spectrum still shows the same −ve/+ve pattern in the signs of the coupled *B* terms to high energy that is seen in the spectra of TNPc(−3) and $[ZnPc(-3)]^-$. Spectral band deconvolution analysis[34] of the low-temperature MCD and absorption spectra of $[ZnPc(-3)]^-$ has indicated that it is much more difficult to assign individual bands to specific transitions in this region of the spectrum as there is significant configurational interaction between the overlapping B1 and B2 transitions and other higher energy transitions. The spectral bandwidths associated with higher energy $\pi \rightarrow \pi^*$ excited states of heteroaromatic molecules are larger than those associated with the lowest energy excited state.[66] Band broadening is particularly significant when there is overlap between the bands associated with different excited states and when there is an underlying $n \rightarrow \pi^*$ state. The deconvolution analysis of $[ZnPc(-3)]^-$ indicated that spectral bands associated with $n \rightarrow \pi^*$ transitions linking the lone pair orbitals of the aza nitrogens with empty π^* orbitals may overlap with the bands associated with the $\pi^* \rightarrow \pi^*$ transition.[34] The impact of partial aza substitution and dimerization is therefore less apparent in the B1/B2 region than in the lower energy Q and $\pi^* \rightarrow \pi^*$ regions of the spectrum as changes in the B1/B2 region are masked by the effects of configurational interaction between the higher energy excited states.

Conclusions

The optical spectra of TBTrAP and TNTrAP are similar to those of analogous phthalocyanine complexes. The spectral bands can thus be assigned on the basis of the band assignments developed for the phthalocyanines. ZINDO calculations indicate that the main impact of partial aza substitution at the bridging 5-, 10-, 15-, and 20-positions is to alter the degree of separation between the first and second HOMO's of the π-system. The MCD spectrum of the TBTrAP anion radical species is, however, markedly different from those that have been reported for the phthalocyanines,[3b] as the addition of an electron to TBTrAP leads to the formation of a dimeric species. The optical transitions of the anion radical spectra can be assigned satisfactorily within the framework of the assignment that was previously developed for metal phthalocyanine anion radicals.[34] The development of detailed MO calculations that can fully account for the $\pi \rightarrow \pi^*$, $\pi^* \rightarrow \pi^*$, and $n \rightarrow \pi^*$ bands seen in the absorption and MCD spectra of both Pc and TBTrAP anion radical species would result in a greatly improved understanding of the electronic structure of porphyrin and phthalocyanine complexes.

Acknowledgment. We thank Dr. Aitken Hoy for his help with the EPR measurements, and we gratefully acknowledge financial support from the Natural Sciences and Engineering Research Council of Canada and the Academic Development Fund at UWO (to C.C.L. and M.J.S.), the Province of Ontario for a Differential Fee Bursary (to J.M.), and the Asahi Glass Foundation (to N.K.). M.J.S. acknowledges travel support as a fellow of the Japanese Society for the Promotion of Science during this work. M.J.S. is a member of the Centre for Chemical Physics and the Photochemistry Unit at the University of Western Ontario and acknowledges their continued support of this work. This is publication No. 536 of the Photochemistry Unit.

Supporting Information Available: Tables 5 and 6, providing the calculated spectral data for H_2TBTrAP and H_2TNTrAP from the ZINDO program, and Figures 10 and 11, illustrating the energies of the calculated MO's (7 pages). Ordering information is given on any current masthead page.

IC961389N

(66) Hochstrasser, R. M.; Marzzacco, C. *J. Chem. Phys.* **1968**, *49*, 971.
(67) (a) Piepho, S. B.; Schatz, P. N. *Group Theory in Spectroscopy with Applications to Magnetic Circular Dichroism*; Wiley: New York, 1983. (b) Stephens, P. *J. Adv. Chem. Phys.* **1976**, *35*, 197.